Carbohydrate Research, 192 (1989) 197–214
Elsevier Science Publishers B.V., Amsterdam – Printed in The Netherlands

A PHYSICO-CHEMICAL ASPECT OF CYANINE DYE–CYCLOMALTO-OLIGOSACCHARIDE SYSTEMS: ENHANCED DIMERIZATION OF THE DYE AND SHORTENING OF THE LIFETIME OF THE PHOTOISOMER*

KAZUO KASATANI†, MASAFUMI OHASHI, AND HIROYASU SATO‡
Chemistry Department of Resources, Faculty of Engineering, Mi'e University, Tsu 514 (Japan)
(Received December 29th, 1988; accepted for publication, May 2nd, 1989)

ABSTRACT

Cyclomaltoheptose (βCD) and cyclomalto-octaose (γCD) enhance the dimerization of some cyanine dyes in aqueous solution. The presence and absence of the enhancement is governed by the length of the linking chain, the presence or absence of a bulky atom on the chain, and the size of the chromophore at each end. These CDs accelerate the back-reaction of the photoisomer of some cyanine dyes to the original conformer. The transient absorbance of the photoisomer shows a single-exponential decay, indicating rapid equilibration of the photoisomer included in the CD cavity and that in solution. For each of the dye–CD pairs with enhanced dimerization, the lifetime of the photoisomer is shortened but the reverse does not always obtain. The shortening of the lifetime of the photoisomer involves the monomer dye included in the cavity of the CD.

INTRODUCTION

The ability of cyclomalto-oligosaccharides (cyclodextrins, CDs) to include a wide variety of organic molecules in their cavities[3,4] provides the basis for physico-chemical phenomena that are sensitive to molecular association, such as monomer–dimer equilibria or the formation of molecular complexes[5,6]. In some cases, molecular association in the electronic excited states, *e.g.*, formation of an excimer or exciplex[7,8], can be induced. CDs can also influence the conformational equilibria of molecules[9]. When a CD affects the relative stabilities of conformers in the excited state, modification of photochemical reactivity, *e.g.*, that in *cis-trans* isomerization of azobenzene[10] or Norrish type I/type II behavior of alkyldeoxybenzoins[11], occurs.

Cyanine dyes are used as photographic sensitizing materials[12], mode-locking

*Reported briefly in refs. 1 and 2.
†Present address: Department of Chemistry, Fukuoka Women's University, Fukuoka 813, Japan.
‡Author for correspondence.

0008-6215/89/$ 03.50

and lasing media for lasers[13], *etc.*, and many of their physical and chemical properties are sensitive to the environment. The monomer–dimer (or higher aggregate) equilibrium is sensitive to the presence of salts, organic solvents[14], or such anionic detergents as sodium dodecylsulfate (SDS)[14,15]. The photochemistry of cyanine dyes is also influenced by the molecular environment. The fluorescence and photoisomerization quantum yields depend strongly on the viscosity of solvents[16]. These environmental effects play a key role in the effective practical use of cyanine dyes.

We now report on the effect of cyclomalto-hexaose (αCD), -heptaose (βCD), and -octaose (γCD) on the states of aggregation and the lifetimes of the photoisomers of the cyanine dyes **1–14**.

EXPERIMENTAL

Samples. — 3,3′-Diethyloxacarbocyanine iodide (**1**, DOC), 3,3′-diethyloxadicarbocyanine iodide (**2**, DODC), 3,3′-diethyloxatricarbocyanine iodide (**3**, DOTC), 3,3′-diethylthiacarbocyanine iodide (**4**, DTC), 3,3′-diethylthiadicarbocyanine iodide (**5**, DTDC), 3,3′-diethylthiatricarbocyanine iodide (**6**, DTTC), 1,3,3,1′,3′,3′-hexamethylindocarbocyanine iodide (**7**, HIC), 1,3,3,1′,3′,3′-hexamethylindodicarbocyanine iodide (**8**, HIDC), and 1,3,3,1′,3′,3′-hexamethylindotricarbocyanine iodide (**9**, HITC) (laser grade) were obtained from Dojin. 10-Chloro-3,3′-diethyloxadicarbocyanine iodide (**10**, NK-1165), 6,7,6′,7′-dibenzo-3,3′-diethyloxadicarbocyanine iodide (**11**, NK-2034), 3,3′-diethyl-5,5′-diphenyloxadicarbocyanine iodide (**12**, NK-2035), 5,5′-dichloro-3,3′-diethyloxadicarbocyanine iodide (**13**, NK-2038), and 3,3′-dipropyloxadicarbocyanine iodide (**14**, NK-2606) were obtained from the Japanese Research Institute for Photosensitizing Dyes, Co. αCD and βCD (Nakarai) and γCD (Tokyo Kasei) were used as received. Water was distilled twice.

Absorption spectra. — A Hitachi 200-20 recording spectrophotometer was used at room temperature on aqueous solutions of dye at 5×10^{-5}–5×10^{-6}M, and of CD of 5×10^{-3}M, unless stated otherwise.

Transient absorption and its decay. — The transient absorption was monitored at 632.8 nm with a He–Ne laser (Spectra-Physics 155, 0.95 mW), following pulsed excitation of the dye using a flash-lamp-pumped dye laser (width, ~1 Å; power, ~1 mJ/pulse; pulse width, ~0.8 μs; repetition rate, 6 Hz) with Rhodamine-6G (Kanto, laser grade) as a lasing dye. The exciting wavelength was 600 nm. The monitoring light was passed through the sample cell (Pyrex, 10 × 10 mm) coaxially with the exciting light by the use of a beam-splitter. The attenuation of the monitoring light was measured as a function of time after the exciting laser pulse with a PIN photodiode (Hamamatsu Photonics S-1188). The scattered exciting light was cut by a glass filter (Toshiba R-62). The signal was fed through a pre-amplifier to a transient memory averager (Kawasaki Electronica, M-50/TMC-400), then analyzed by a microcomputer, and displayed on a chart recorder. The concentration of the dye was 10^{-5}M for **2** (DODC), and 2×10^{-5}M for the other dyes.

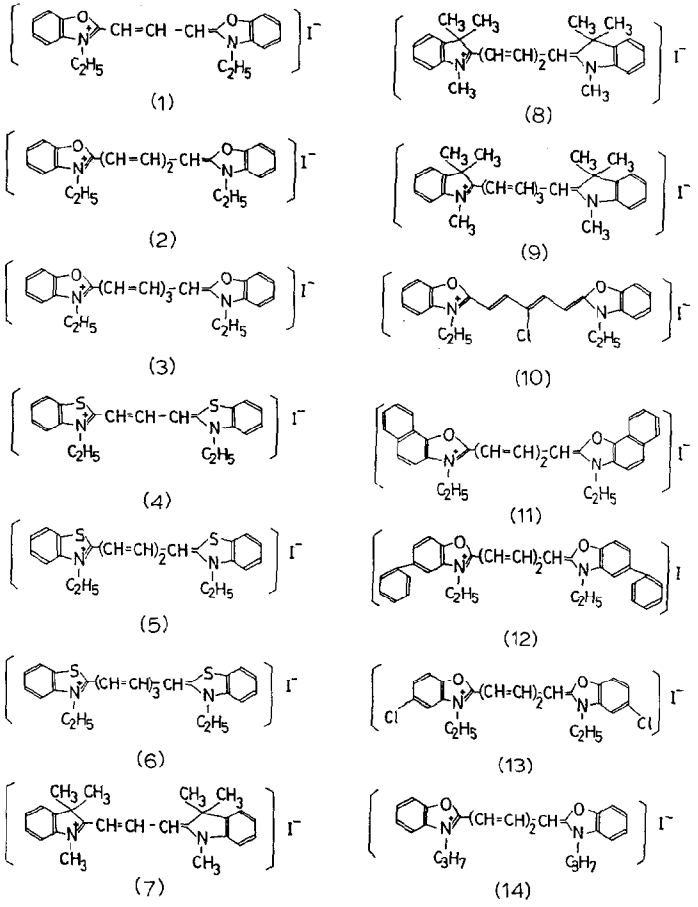

For **5** (DTDC) and **8** (HIDC), which have the absorption band of the original conformer at the monitoring wavelength (632.8 nm), the rate of decay of the photoisomer was measured by the recovery of the absorption of the original conformer. The exciting light was cut by using a monochromator (Nikon G-250). The dye concentrations used were 8×10^{-6} and 2×10^{-6}M for **5** and **8**, respectively, and [CD] was 5×10^{-3}M. The temperature of the sample solution was controlled by using a jacketted cell. The transient absorption spectra of **2** (DODC) were measured by a flash-photolysis apparatus, using a cell with a path length of 10 cm; [**2**] was 5×10^{-7}M.

Molecular mechanics calculations. — An MM2 program was used with FACOM-760 and FACOM-780 computers set up in the Mi'e University Information Processing Center and Nagoya University Computing Center, respectively.

TABLE I

THE ENHANCED DIMERIZATION BY αCD, βCD, AND γCD

Dye	*αCD (4.5 Å)*[a]	*βCD (7.0 Å)*[a]	*γCD (8.5 Å)*[a]
1 (DOC)	x[b]	x	○
2 (DODC)	x	○	○
3 (DOTC)	x	○	○
4 (DTC)	x	x	○
5 (DTDC)	x	x	○
6 (DTTC)	x	○	○
7 (HIC)	x	x	x
8 (HIDC)	x	x	x
9 (HITC)	x	○	○
10 (NK-1165)	x	x	○
12 (NK-2035)	x	○	○
13 (NK-2038)	x	○	○
14 (NK-2606)	x	x	○

[a]Diameter of cavity; ref. 3. [b]x, no enhancement; ○, enhancement.

RESULTS AND DISCUSSION

Enhanced dimerization. — Absorption spectra of the **10**-γCD system for various concentrations of γCD are shown in Fig. 1. The absorption band observed in the absence of γCD is the monomer band, since the dye concentration is low (10^{-5}M), and increase of the concentration of dye resulted in the appearance of the dimer band at shorter wavelength and concomitant weakening of the monomer band. The dimer band of the dye appeared on the addition of γCD. Examples of absorption spectra of some dye–CD systems are shown in Fig. 2. Enhanced dimerization is shown by the appearance of the dimer band on the addition of the CD. The results are summarized in Table I.

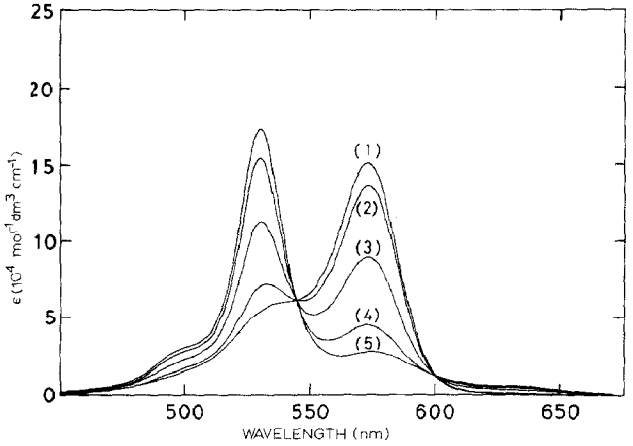

Fig. 1. Absorption spectra of the **10**–γCD system: [**10**] 10^{-5}M, [γCD] 0 (1), 10^{-5}M (2), 10^{-4}M (3), 10^{-3}M (4), 10^{-2}M (5).

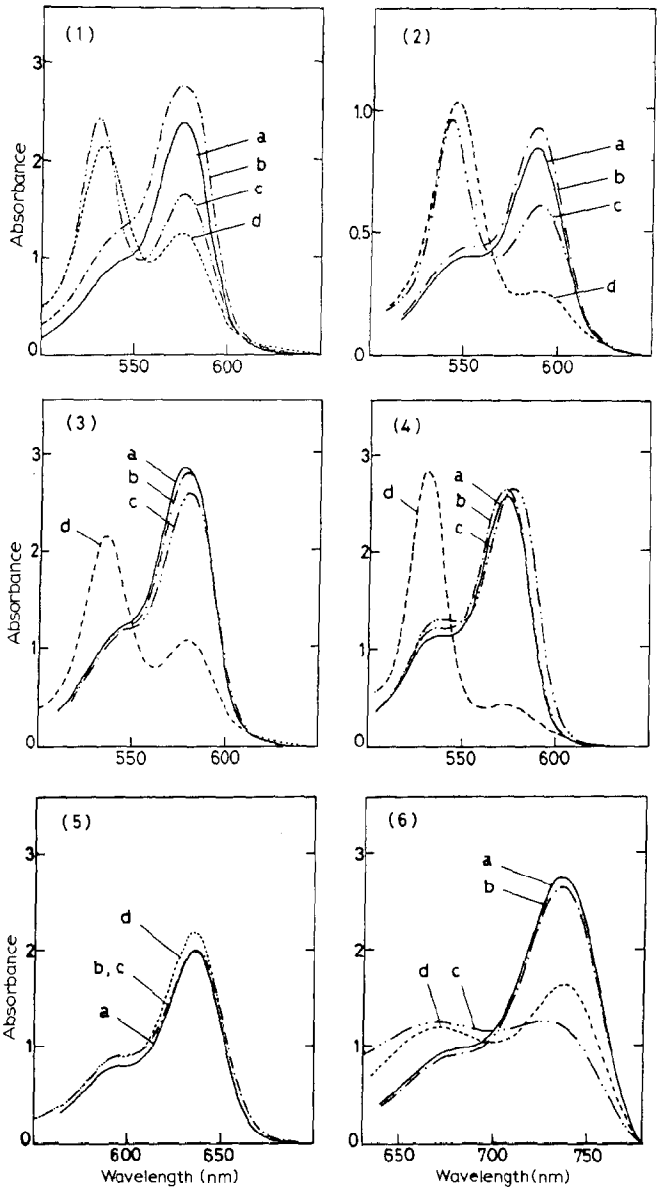

Fig. 2. Absorption spectra of some dye–CD systems: (1) **2** (DODC), (2) **12** (NK-2035), (3) **14** (NK-2606), (4) **10** (NK-1165), (5) **8** (HIDC), (6) **9** (HITC). Curves a–d are without CD, with αCD, with βCD, and with γCD, respectively: dye, 2×10^{-5}M; CD, 5×10^{-3}M.

As is clear from the data in Table I, αCD does not enhance dimerization, presumably because the diameter of the cavity[3] (0.45 nm) is too small. In contrast, γCD (diameter of cavity[3], 0.85 nm) enhances dimerization for most of the dyes studied, and its failure for **7** and **8** can be ascribed to the presence of bulky end-groups. However, γCD enhances the dimerization of **9**, which has the same end-group as **7** and **8**, but a longer linking chain. The enhancement of dimerization by βCD (diameter of cavity[3], 0.70 nm) does not occur for dyes with a CH=CH-CH linking group (**1, 4**, and **7**), a bulky end-group (**8**), a sulfur atom on the indole ring (**5**), an *N*-propyl group (**14**), or a bulky atom in the linking chain (**10**). Thus, the occurrence of dimerization is governed by steric factors and, empirically, appears not to occur for dyes with (*a*) a bulky end-group or a bulky atom on the linking chain, and (*b*) a short linking group. Thus, steric hindrance seems to be an important factor in the formation of an inclusion compound. Comparison of **5** and **6** (or **8** and **9**) suggests that the bulky end-group that hinders the enhancement of dimerization for the dye with the shorter linking group (**5** or **8**) does not hinder it for the dye with the longer linking group (**6** or **9**).

Many cyanine dyes form dimers or higher aggregates in concentrated solutions. For many typical cyanine dyes, the decrease in free energy upon aggregation is relatively small, so that small changes in the properties of the solvent or the presence of organic additives affects the aggregation equilibria[12]. Additives such as urea, phenols, alcohols, *etc.* diminish the effective dielectric constant of a solvent and enhance the repulsion between similarly charged dye ions, resulting in their deaggregation[14]. The deaggregation of rhodamine B, a xanthene dye, by βCD has been observed[17] in an aqueous solution with the enhancement of the laser action of the dye. Two molecules of anthracene sulfonate can be included[6] in the cavity of γCD. Two molecules of Crystal Violet, Methylene Blue, and Methyl Orange can be included[18] in the cavity of γCD, but only one in that of βCD. 2:2 Inclusion complexes have been reported[19] for the systems naphthalene–βCD and 2-methoxynaphthalene–βCD. In the present study, the dimerization of some cyanine dyes was enhanced by the addition of βCD or γCD.

*Distribution of monomer DODC (**2**) between the aqueous phase and the cavity of βCD.* — There were only small changes in the spectra (Fig. 2) when the concentration of βCD was varied for a fixed concentration of dye, and these could be attributed to changes in the polarity of the solvent. Remarkable enhancement of fluorescence has been reported[20] for aqueous solutions of some benzene derivatives on the addition of CD and this effect was used to determine the equilibrium constant. However, there was little change in the fluorescence quantum yield (ϕ_F) of the monomer dye **2** on the addition of βCD. The non-radiative decay of the first excited singlet (S_1) state of **2** in solution at room temperature is dominated by the photoisomerization process, because the quantum yield of the inter-system crossing to the triplet state is low ($\phi_T < 5 \times 10^{-3}$ in ethanol)[21] and because the $S_1 \rightarrow S_0$ internal conversion is not important compared to the photoisomerization at room temperature and above[22]. Therefore, little change in ϕ_F implies little effect of βCD

on the photoisomerization in the S_1 state. However, βCD accelerates the back-reaction of the photoisomer to the original conformer in the ground state, as shown below by the shortening of the lifetime of the photoisomer. An alternative, and more probable, explanation is that monomers of the original conformer of **2** are present almost exclusively in the aqueous phase. In other words, the equilibrium **2** + βCD ⇄ **2**–βCD is shifted markedly to the left. It is difficult to believe that the monomer **2** is hardly incorporated in the CD cavity of βCD, whereas the dimer is incorporated. However, the simulation of the absorbance at the wavelength of dimer absorption band *vs.* [βCD] (shown below) indicates that the concentration of monomer dye incorporated in the cavity of βCD is much smaller than that of the monomer dye in the solution.

Type of dimer for DODC (2). — There are two possible types of dimer, namely, D_2–CD and D_2–$(CD)_2$. In order to determine the identity of the dimer, the variation of the absorbance at the wavelength of the dimer band for various concentrations of βCD, with a fixed concentration of **2**, was studied. The resulting curve was analyzed as follows:

(*a*) *D_2–CD.* The relevant equilibrium is

$$2D + 2CD \overset{K_1}{\rightleftarrows} 2(D\text{–}CD) \overset{K_2}{\rightleftarrows} D_2\text{–}CD + CD \qquad (1)$$

$$K_1 = [D\text{–}CD]/\{[D][CD]\} \qquad (2)$$

$$K_2 = [D_2\text{–}CD][CD][D\text{–}CD]^2 \qquad (3)$$

$$K_1^2K_2 = [D_2\text{–}CD]/[D]^2[CD] \qquad (4)$$

Equations 5 and 6 hold for these concentrations and the total initial concentrations $[D_0]$ and $[CD_0]$,

$$[D_0] = [D] + [D\text{–}CD] + 2[D_2\text{–}CD] \qquad (5)$$

$$[CD_0] = [CD] + [D\text{–}CD] + [D_2\text{–}CD] \qquad (6)$$

where the concentration of dimer in the aqueous phase, $[D_2]$, can be neglected, since the total concentration of dye is low and the dimer band does not appear without the addition of CD.

The absorbance at the dimer band is

$$A = (\varepsilon_D[D] + \varepsilon_{D\text{–}CD}[D\text{–}CD] + \varepsilon_{D_2\text{–}CD}[D_2\text{–}CD])L, \qquad (7)$$

where ε is the relevant molar extinction coefficient and L is path length.

From these relations, the A *vs.* [CD] curves in Fig. 3 can be simulated, taking

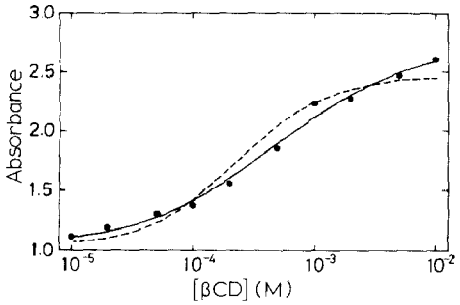

Fig. 3. The dependence of absorbance at the wavelength of the dimer band of **2** (DODC) in the **2**–βCD system as a function of [βCD] (●), and its simulation assuming two models for CD-enhanced formation of dimer: ——, model (*a*); and ------, model (*b*) (See text).

ε_{D_2-CD}, K_1, and K_2 as adjustable parameters and assuming that $\varepsilon_{D-CD} = \varepsilon_D$. The best-fit result is shown by the solid line in Fig. 3. The best-fit [CD], [D], [D–CD], and [D_2–CD] for each [CD_0] are given in Table II. The equilibrium value of [D–CD] is small (by approximately one order of magnitude) compared with that of [D_2–CD].

(*b*) *D_2–CD_2.* A similar treatment for the equilibrium

$$2D + 2CD \overset{K_1'}{\rightleftarrows} 2(D\text{–}CD) \overset{K_2'}{\rightleftarrows} D_2\text{–}CD_2 \qquad (8)$$

and absorbance

$$A = (\varepsilon_D[D] + \varepsilon_{D-CD}[D\text{–}CD] + \varepsilon_{D_2-CD_2}[D_2\text{–}CD_2])L \qquad (9)$$

TABLE II

BEST-FIT VALUES OF [CD], [D], [D–CD], AND [D_2–CD] IN EQUILIBRIUM FOR EACH VALUE OF [CD_0] BY SIMULATION (*a*) (M) (SEE TEXT)

$[CD_0]$	$[CD]$	$[D]$	$[D\text{–}CD]$	$[D_2\text{–}CD]$
1×10^{-5}	9.75×10^{-6}	1.98×10^{-5}	6.90×10^{-9}	2.39×10^{-7}
2×10^{-5}	1.95×10^{-5}	1.94×10^{-5}	1.35×10^{-8}	4.57×10^{-7}
5×10^{-5}	4.90×10^{-5}	1.82×10^{-5}	3.18×10^{-8}	1.02×10^{-6}
1×10^{-4}	9.82×10^{-5}	1.68×10^{-5}	5.88×10^{-8}	1.73×10^{-6}
2×10^{-4}	1.97×10^{-4}	1.48×10^{-5}	1.04×10^{-7}	2.70×10^{-6}
5×10^{-4}	4.96×10^{-4}	1.17×10^{-5}	2.06×10^{-7}	4.21×10^{-6}
1×10^{-3}	9.94×10^{-4}	9.28×10^{-6}	3.29×10^{-7}	5.34×10^{-6}
2×10^{-3}	1.99×10^{-3}	7.14×10^{-6}	5.07×10^{-7}	6.33×10^{-6}
5×10^{-3}	4.99×10^{-3}	4.84×10^{-6}	8.62×10^{-7}	7.30×10^{-6}
1×10^{-2}	9.99×10^{-3}	3.53×10^{-6}	1.26×10^{-6}	7.76×10^{-6}

leads to the best-fit simulation curve presented by the broken line in Fig. 3.

The results of these simulations favour the formation of D_2–CD. The values of best-fit K_1, K_2, and ε_{D_2-CD} in the simulation (*a*) are 36 M^{-1}, 4.9×10^4, and 6.0×10^5 $M^{-1}.cm^{-1}$, respectively. The value of $K_1^2K_2$ (6×10^7 M^{-2}) is comparable to the corresponding value[18] (2×10^7 M^{-2}) for γCD–(Crystal Violet)$_2$.

The simulation curve for (*b*) does not reproduce well the experimental points. The curvature in the lower and higher ranges of [βCD] is too large, and the rising tendency of experimental points in the highest concentration range is not reproduced. Moreover, the experimental data on the enhanced dimerization, mentioned above in the form of an empirical rule, argue against the D_2–$(CD)_2$ structure. The fact that aggregation was observed only for dyes with sufficiently long linking chains and/or non-bulky end-groups strongly suggests that the connecting chain is contained within the cavity of the CD and the end groups are located outside. Since the linking chains cannot thread two CDs, the D_2–$(CD)_2$ structure is ruled out.

Molecular mechanics calculations. — The incorporation of two molecules of dye in the cavity of βCD is feasible energetically when the destabilization due to expansion of the CD annulus is compensated by the gain in energy due to hydrophobic stabilization plus dimerization of the dye. This aspect has been studied by molecular mechanics (MM) calculations[23].

A preliminary calculation has been made of the stabilization energy for the reaction of DOTC (**3**), **3**–βCD + **3** → (**3**)$_2$–βCD using the MM2 program. The reaction co-ordinate was chosen as shown in Fig. 4. One of the two molecules of **3** is fixed in the cavity of the βCD and the other approaches the cavity along the x axis. The molecular geometry of the total system (including βCD) was optimized for each value of x. The calculation took into account van der Waals and dipole–dipole interactions but not the positive charge on **3**, which causes charge–charge and charge–dipole interactions, the effect of hydrogen bonding, and the effect of the surrounding water molecules. The calculated total energy of the system is shown in Fig. 5 as a function of x (Å). The total energy decreases as the second molecule of **3** approaches the **3**–βCD complex. However, a potential barrier (~50 $kJ.mol^{-1}$) appears at the position where the bulky head group of the second molecule enters the cavity of the βCD. The optimized molecular geometries at the positions a–c in Fig. 5 are given in Fig. 6. As the bulky head group of **3** enters the cavity of the βCD (*i.e.*, b in Fig. 6), the annulus of the βCD expands in one direction and shrinks in the other. The calculation gives a stabilization energy (the energy gain on the accommodation of the second molecule of **3** in the cavity of the βCD) as large as ~170 $kJ.mol^{-1}$ (Fig. 5). The experimental value of ΔH for the reaction **10**–γCD + **10** → (**10**)$_2$–γCD is ~31 $kJ.mol^{-1}$. Therefore, a more realistic value of the stabilization energy for the reaction **3**–βCD + **3** → (**3**)$_2$–βCD may be in the range 20–40 $kJ.mol^{-1}$. The large value of the calculated stabilization energy is probably due to neglect of the factors mentioned above, particularly the positive charge on **3**. Moreover, inclusion of positively charged **3** in the cavity of βCD causes

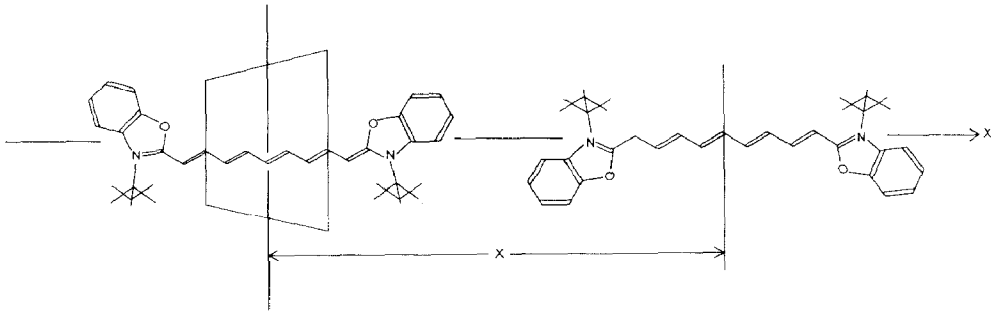

Fig. 4. The reaction co-ordinate used in the molecular mechanics calculation of the reaction **3**–βCD + **3** → (**3**)$_2$–βCD.

a significant loss of stabilization of the dye in the polar aqueous phase. Improvements of the calculations are being studied. However, the height of the barrier, ~50 kJ.mol^{-1}, is dominated by steric hindrance and, therefore, its value must be essentially free from the factors neglected in the present calculation. Such a barrier seems to be small enough to be surmounted. Therefore, the formation of (**3**)$_2$–βCD is allowable on energy grounds. A similar situation can be expected for the other dyes.

Transient absorption due to the photoisomer of **2** *(DODC).* — The photoisomerization of cyanine dyes in fluid media has been studied in relation to their mode-locking action[17]. The photoisomer has a characteristic transient absorption band at a wavelength longer than that of the orginal conformer. For **2**, the peak of the transient absorbance of the photoisomer in aqueous solution appears near 615 nm (*cf.* 575 nm for the original conformer). In the presence of 5 × 10^{-3}M βCD, the peak of the transient absorption shifted to 617 nm (*cf.* ~620 nm in ethanol[21]).

Decay of the transient absorption of **2**. — The observed decay of the transient absorbance of **2** in the **2**–βCD system was single exponential for 2 × 10^{-2}M βCD at 10–30°. The rate of decay increased with increase in [βCD] as shown in Fig. 7. The

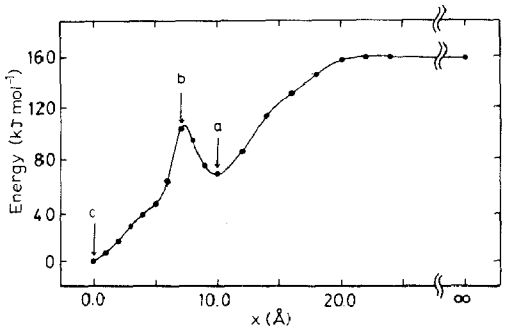

Fig. 5. Total energy obtained by the molecular mechanics calculation on the reaction **3**–βCD + **3** → (**3**)$_2$–βCD. Arrows a–c correspond to the three types of molecular geometry shown in Fig. 6.

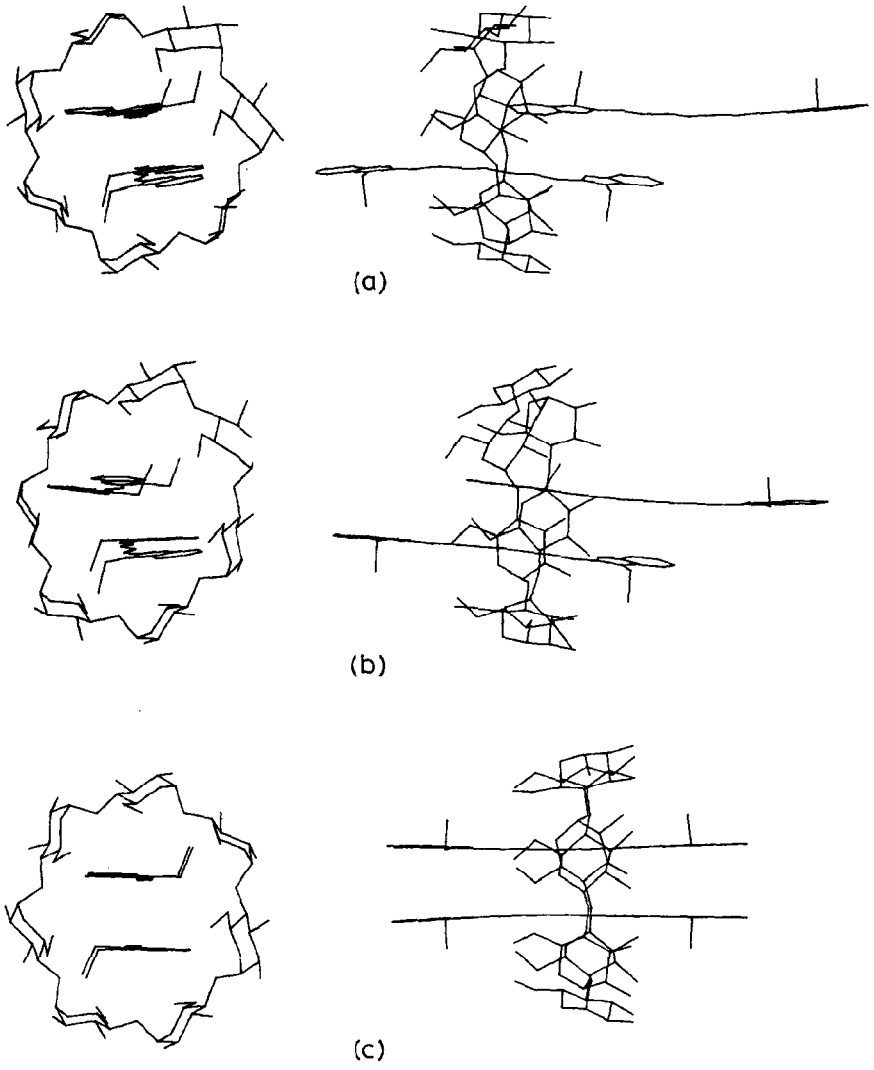

Fig. 6. Optimized molecular geometry for a–c in Fig. 5. Note the large distortion of the βCD ring in b.

rates of decay for the **2**–αCD and **2**–γCD systems are given in Fig. 8. Apparently, αCD does not affect the rate of decay and the effect of γCD is comparable to that of βCD.

Mechanism of the photoisomerization of **2**. — The mechanism of the photoisomerization of cyanine dyes in their first excited singlet (S_1) states has been studied in considerable detail. Schematic potential energy curves can be drawn[22,24,25] that are characterized by a potential barrier which the photoisomer in the ground state surmounts in the back-reaction. The rate of the back-reaction depends on the viscosity of the solvent[16].

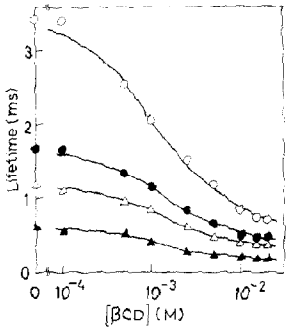

Fig. 7. Dependence of the lifetimes of the photoisomer of **2** on [βCD]: [**2**] 10^{-5}M; ○, 10.2°; ●, 17.9°; △, 22.0°; ▲, 32.3°. The solid lines are simulated curves.

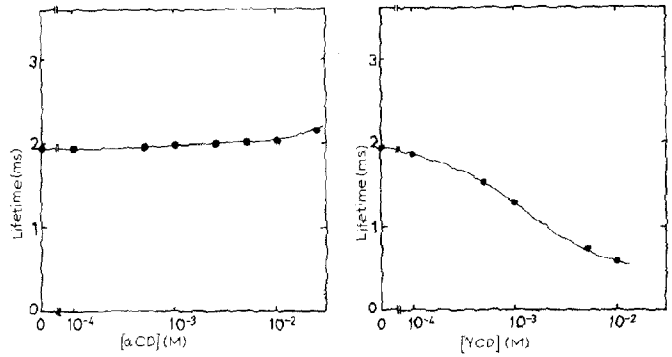

Fig. 8. Dependence of the lifetimes of the photoisomer for the **2**–αCD and **2**–γCD systems on [CD]: [**2**] 10^{-5}M, 16.7°.

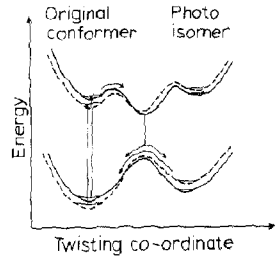

Fig. 9. A schematic model for the photophysics of **2** (DODC). Solid lines, **2** in the aqueous phase (**D** or **P** in the text); broken lines, **2** in the inclusion complex with βCD (D–CD or P–CD in the text).

Two sets of potential energy curves must be considered relevant to dye molecules in aqueous solution and in the cavity of the CD. Schematic potential energy curves are shown in Fig. 9. Some of the original conformer of the dye (D) in the aqueous solution is excited and gives the photoisomer dye (P) in the ground state, and some (D–CD) in the cavity of the CD is excited and gives the photoisomer dye (P–CD) in the ground state in the cavity. In the following scheme,

$$\begin{array}{ccc} & \overset{k_1}{} & \\ \mathrm{P} + \mathrm{CD} & \rightleftarrows & \mathrm{P{-}CD} \\ & \underset{k_{-1}}{} & \\ \downarrow k_w & & \downarrow k_{CD} \\ \mathrm{D} + \mathrm{CD} & & \mathrm{D{-}CD} \end{array}$$

k_1 and k_{-1} are the rate constants for the association and dissociation of the photoisomer and βCD, respectively, and k_w and k_{CD} are those for the respective back-reactions. The rate equations for P and P–CD are

$$\mathrm{d[P]}/\mathrm{d}t = k_{-1}[\mathrm{P{-}CD}] - (k_w + k_1[\mathrm{CD}])[\mathrm{P}] \qquad (10)$$

$$\mathrm{d[P{-}CD]}/\mathrm{d}t = k_1[\mathrm{P}][\mathrm{CD}] - (k_{CD} + k_{-1})[\mathrm{P{-}CD}] \qquad (11)$$

A double exponential decay, with the decay constants k_w and k_{CD}, is expected because P and P–CD have an overlapping transient absorption at the monitoring wavelength. However, only a single exponential decay was observed for the **2**–βCD system for the range of [βCD] studied. The observed rate of decay increased with the increase in [βCD].

The relevant kinetics can be analysed by reference to the treatments[26,27] on the decay of phosphorescence in the presence of association–dissociation equilibria between phosphorescence probes and micelles, and that[28] associated with inclusion equilibria of phosphorescent detergents in the cavities of βCD and γCD. If steady-state conditions are assumed for [P], *i.e.*,

$$\mathrm{d[P]}/\mathrm{d}t = 0,$$

then, from equation *10*,

$$[\mathrm{P}] = k_{-1}[\mathrm{P{-}CD}]/(k_w + k_1[\mathrm{CD}]) \qquad (12)$$

The fractions (a and $1 - a$, respectively) of P–CD and P are given, respectively, by

$$a = (k_w + k_1[\mathrm{CD}])/(k_w + k_1[\mathrm{CD}] + k_{-1}) \qquad (13)$$

and

$$1 - a = k_{-1}/(k_w + k_1[CD] + k_{-1}) \quad (14)$$

The steady-state treatment on [P–CD] gives corresponding formulae which include k_{CD}. The observed decay is for the total of [P–CD] and [P], and is given as

$$\begin{aligned} &- d([P\text{–}CD] + [P])/dt = k_{CD}[P\text{–}CD] + k_w[P] \\ &= \{ak_{CD} + (1 - a)k_w\}([P\text{–}CD] + [P] \end{aligned} \quad (15)$$

The rate constant for the decay is

$$1/\tau = \{k_{CD}(k_w + k_1[CD]) + k_w k_{-1}\}/(k_w + k_1[CD] + k_{-1}). \quad (16)$$

Assuming, in addition, that $k_1[CD]$ and k_{-1} are much larger than k_w or k_{CD} gives, instead of equation *12*,

$$[P] = k_{-1}[P\text{–}CD]/k_1[CD]$$

or

$$[P\text{–}CD]/[P][CD] = k_1/k_{-1} = K \quad (17)$$

The fractions of P–CD and P are now given as

$$a = K[CD]/(K[CD] + 1) \quad (18)$$

$$1 - a = 1/(K[CD] + 1) \quad (19)$$

The equation for the decay of [P–CD] + [P] changes accordingly, and the decay rate constant is

$$\begin{aligned} 1/\tau &= ak_{CD} + (1 - a)k_w \\ &= (k_{CD}K[CD] + k_w)/(K[CD] + 1) \end{aligned} \quad (20)$$

The values reported[28,29] for the rate of complexation, k_1, fall in the range of 10^7–10^9 $M^{-1}.s^{-1}$. Since $[CD] = 5 \times 10^{-3}$M, the values of $k_1[CD]$ should be 10^4–10^7 s^{-1}. The reported[28] values of the rate of decomplexation, k_{-1}, are 10^5–10^6 s^{-1}. Therefore, the values of $k_1[CD]$ and k_{-1} can be considered to be large enough to support the above assumption.

Shortening of the lifetime of the photoisomer of **2** *on inclusion in the cavity of βCD.* — Based on the model presented here, the curves for the observed rate of decay *vs.* [βCD] for a fixed [**2**] in Fig. 7 were simulated, taking k_{CD} and K as adjustable parameters. The k_w values used were those corrected for the increase in the viscosity of the solvent by adding βCD as follows. There was a small extension

of the lifetime of the photoisomer on the addition of αCD, which does not include the dye (*e.g.*, 2.04 ms for [αCD] 10mM; *cf.* 1.96 ms in water, at 16.7°). This effect can be attributed to a small increase in the viscosity of the solvent. The $k_w = \tau_w^{-1}$ values used in the simulation were those measured in the presence of αCD, at the same concentration and temperature as for βCD.

Activation energies and thermodynamic quantities for **2**. — The values of $\tau_{CD} = k_{CD}^{-1}$ obtained by this simulation are plotted in Fig. 10 against reciprocal temperature, in comparison with $\tau_w = k_w^{-1}$ (experimental values for an aqueous solution) and $\tau_{SDS} = k_{SDS}^{-1}$ (experimental values in 10^{-2}M SDS). The activation energies of the back-reaction obtained from this Arrhenius plot were 45 ±2, 54 ±2, and 65 ±2 kJ.mol^{-1} for the P → D process in the cavity of βCD, in water, and in solution in the presence of SDS, respectively. These values are similar. The values of the equilibrium constants K increase with temperature as shown in Fig. 11, which shows that P–CD is less stable than P + CD. Using the relation

$$\Delta G = \Delta H - T\Delta S = -RT\ln K \qquad (21)$$

the enthalpy and entropy changes ΔH = 12 ±2 kJ.mol^{-1} and ΔS = 84 ±7 J.mol^{-1}K^{-1} were obtained. The instability of P–CD compared to P + CD is the result of increased steric repulsion on photoisomerization.

Does the enhanced dimerization affect the shortening of the lifetime of the photoisomer of **2**? — As discussed above, the enhancement of dimerization and the shortening of the lifetime of the photoisomer occur for the **2**–βCD system. If the dimer dye (D_2–CD) incorporated in the cavity of βCD gives the photoisomer to any substantial extent, the process D_2–CD + $h\nu$ → DD*–CD → DP–CD will be important and the equilibrium DP–CD ⇄ P–CD + D or DP–CD ⇄ D–CD + P in the electronic ground state must be taken into account (the asterisk connotes the excited state). The kinetics of the decay of the photoisomer will be affected then by the equilibrium D–CD + D ⇄ D_2–CD. However, this is not so, because the observed rate of decay of the photoisomer was invariant with the change of [**2**] and excitation wavelength from the monomer to the dimer band for a fixed [βCD]. This

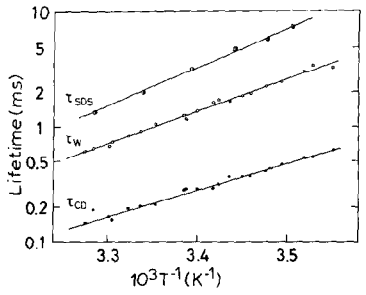

Fig. 10. Arrhenius plot of τ_w (○), τ_{CD} (●), and τ_{SDS} (◑) for the **2**–βCD system.

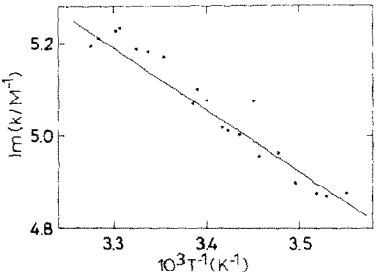

Fig. 11. Temperature dependence of the equilibrium constant K for the **2**–βCD system.

finding can be explained by assuming that the quenching of D* in DD*–CD to give D_2–CD is much faster than the non-radiative path DD*–CD → DP–CD, or that DD*–CD quickly loses one dye molecule to give D*–CD or D–CD. Each process would result in a small steady-state concentration of DP–CD.

It is concluded that the dye molecules involved in the photoisomerization process are essentially those incorporated in the cavity of the CD as a monomer.

Shortening of the lifetimes of the photoisomers of the other dye–CD pairs. — The results are given in Table III, together with those for **2**. αCD does not affect the lifetime, which indicates that not even the monomers of these dyes are included. βCD or γCD shortened the lifetimes of the photoisomers of all of the dyes, except **5**–βCD. The shortening of the lifetimes implies that the dye monomer can be incorporated in the cavity of the CD. The lifetimes of the photoisomers were longer for γCD than for βCD. Although the reciprocal of the observed lifetime must be a weighted average of those of τ_w and τ_{CD} (as in equation *20*), it can be deduced that the value of τ_{CD} for each dye is larger for γCD than for βCD. This result may reflect the smaller steric hindrance on the photoisomer in the wider cavity of γCD.

Comparison of the data in Tables I and III indicates that all of the dye–CD pairs with enhanced dimerization show the shortening of the lifetime of the photo-

TABLE III

SHORTENING OF THE LIFETIMES OF THE PHOTOISOMERS OF VARIOUS DYES BY αCD, βCD, AND γCD AT 20°

Dye[a]	*Without CD*	*αCD*	*βCD*	*γCD*
2 (DODC)	1.54[b]	1.59	0.53	0.47
5 (DTDC)	0.18	0.14	0.13	0.09
8 (HIDC)	0.20	0.22	0.15	0.15
10 (NK-1165)	0.56	0.57	0.16	0.35
11 (NK-2034)	0.66	0.74	0.30	0.35
12 (NK-2035)	1.27	1.31	0.32	0.49
13 (NK-2038)	1.58	1.62	0.41	0.64
14 (NK-2606)	1.69	1.67	0.62	0.49

[a]Concentrations: **5**, 8×10^{-6}M; **8**, 2×10^{-6}M; others, 2×10^{-5}M; CD, 5×10^{-3}M. [b]Observed lifetimes (ms): the reciprocals of those with CD are a weighted average of those of τ_w and τ_{CD} (see equation *20*).

isomer. However, the reverse does not always obtain. The pairs **10**–βCD and **14**–βCD show the shortening of the lifetimes of the photoisomers but no enhancement of the formation of dimers. The structure of these dyes is similar to that of **2**, the only difference being the alkyl group (Et or Pr) on the quaternary nitrogen atom or the presence of a Cl substituent in the linking group. Thus, enhanced dimerization is not a prerequisite for shortening of the lifetime of the photoisomer, and this supports the view that only the monomer dye molecule incorporated in the cavity of the CD is involved in the photoisomerization. The dyes which do not experience enhanced dimerization, but show shortening of the lifetime of the photoisomer, form only a monomer complex with CD. The formation of a monomer or a dimer complex with CD seems to be controlled by steric factors.

ACKNOWLEDGMENTS

We thank Professor Shunji Kato and Dr. Akio Yoshimura (Osaka University) for measurement of the transient absorption, and Messrs. H. Takasaki and A. Takayasu for their assistance in the experiment.

REFERENCES

1 K. KASATANI, M. KAWASAKI, AND H. SATO, *J. Phys. Chem.*, 88 (1984) 5451–5453.
2 K. KASATANI, M. OHASHI, M. KAWASAKI, AND H. SATO, *Chem. Lett.*, (1987) 1633–1637.
3 M. L. BENDER AND M. KOMIYAMA, *Cyclodextrin Chemistry*, Springer, New York, 1977.
4 V. RAMAMURTHY AND D. F. EATON, *Acc. Chem. Res.*, 21 (1988) 300–306.
5 T. YOROZU, M. HOSHINO, AND M. IMAMURA, *J. Phys. Chem.*, 86 (1982) 4426–4429.
6 T. TAMAKI, *Chem. Lett.*, (1984) 53–56; T. TAMAKI AND T. KOKUBU, *J. Inclusion Phenom.*, 2 (1984) 815–822.
7 N. J. TURRO, T. OKUBO, AND G. C. WEED, *Photochem. Photobiol.*, 35 (1982) 325–329.
8 J. EMERT, D. KODALI, AND R. CATENA, *J. Chem. Soc., Chem. Commun.*, (1981) 758–759; G. S. COX AND N. J. TURRO, *J. Am. Chem. Soc.*, 106 (1984) 422–424.
9 R. ARAD-YELLIN AND D. F. EATON, *J. Phys. Chem.*, 87 (1983) 5051–5055.
10 P. BORTOLUS AND S. MONTI, *J. Phys. Chem.*, 91 (1987) 5046–5050.
11 G. D. REDDY AND V. RAMAMURTHY, *J. Org. Chem.*, 52 (1987) 5521–5528.
12 D. M. STURMER AND D. W. HESELTINE, in T. H. JAMES (Ed.), *The Theory of Photographic Process.*, 4th edn., Macmillan, New York, 1977, pp. 194–290.
13 K. H. DREXHAGE, in F. P. SCHAFER (Ed.), *Dye Lasers*, 2nd edn., Springer, Berlin, 1977, pp. 144–193; M. MAEDA, *Rev. Laser Engineering (Osaka)*, 8 (1980) 694–712.
14 A. H. HERZ, *Photogr. Sci. Eng.*, 18 (1974) 323–335.
15 H. SATO, M. KAWASAKI, K. KASATANI, N. NAKASHIMA, AND K. YOSHIHARA, *Bull. Chem. Soc. Jpn.*, 56 (1983) 3588–3594.
16 J. JARAUDIAS, *J. Photochem.*, 13 (1980) 35–48.
17 Y. DEGANI, I. WILLNER, AND Y. HAAS, *Chem. Phys. Lett.*, 104 (1984) 496–499.
18 H. HIRAI, N. TOSHIMA, AND S. UENOYAMA, *Bull. Chem. Soc. Jpn.*, 58 (1985) 1156–1164.
19 S. HAMAI, *Bull. Chem. Soc. Jpn.*, 55 (1982) 2721–2729.
20 M. HOSHINO, M. IMAMURA, K. IKEHARA, AND Y. HAMA, *J. Phys. Chem.*, 85 (1981) 1820–1823.
21 D. N. DEMPSTER, T. MORROW, R. RANKIN, AND G. F. THOMPSON, *J. Chem. Soc., Faraday Trans. 2*, 68 (1972) 1479–1496.
22 S. P. VELSKO AND G. R. FLEMING, *Chem. Phys.*, 65 (1982) 59–70.
23 N. L. ALLINGER AND Y. H. YUH, *Quantum Chemistry Program Exchange (QCPE)*, 13 (1981) 395–397.
24 C. RULLIÈRE, *Chem. Phys. Lett.*, 43 (1976) 303–308.

25 J.-P. FOUASSIER, D.-J. LOUGNOT, AND J. FAURE, *Opt. Commun.*, 23 (1977) 393–397.
26 M. ALMGREN, F. GRIESER, AND J. K. THOMAS, *J. Am. Chem. Soc.*, 101 (1979) 279–291.
27 N. J. TURRO AND M. AIKAWA, *J. Am. Chem. Soc.*, 102 (1980) 4866–4870.
28 N. J. TURRO, T. OKUBO, AND C.-J. CHUNG, *J. Am. Chem. Soc.*, 104 (1982) 1789–1794.
29 R. P. VILLANI, S. F. LINCOLN, AND J. H. COATES, *J. Chem. Soc., Faraday Trans. 1*, 83 (1987) 2751–2756.